[CANCER RESEARCH 63, 8393–8399, December 1, 2003]

Combination Treatment with 17-*N*-Allylamino-17-Demethoxy Geldanamycin and Acute Irradiation Produces Supra-Additive Growth Suppression in Human Prostate Carcinoma Spheroids

Richard Enmon, Wei-Hong Yang, Åse M. Ballangrud, David B. Solit, Glenn Heller, Neal Rosen, Howard I. Scher, and George Sgouros

Memorial Sloan-Kettering Cancer Center, New York, New York

ABSTRACT

Failure to control localized prostate cancer can result not only in localized disease progression but also distant metastatic spread. Whereas significant advances in both surgical technique and radiation therapy have improved local control rates with decreased morbidity, consistent long-term control remains elusive. This study investigates the potential of 17-*N*-allylamino-17-demethoxy geldanamycin (17AAG), a geldanamycin derivative, to sensitize tumor cells to ionizing radiation, permitting a significant improvement to targeted radiotherapies of prostate carcinoma. As a monotherapeutic, 17AAG functions to modulate the action of heat shock protein 90, ultimately affecting a multitude of cellular signaling pathways. It is in Phase I trial and has shown promise in controlling prostate cancer progression. Human prostate tumor cells (LNCaP and CWR22Rv1) were grown as spheroids and incubated for 96 h with increasing doses of 17AAG immediately before and after 2 or 6 Gy low linear energy transfer (LET), high dose-rate irradiation (Cs-137 irradiator). Twelve or 24 spheroids (initial diameter, 150–200 μm) were used per experiment. Response was determined by spheroid volume measurements taken over at least 40 days, after treatment. Incubation of either cell line with 17AAG (≤1000 nM) or irradiation (≤6 Gy) alone resulted in transient median growth delays ranging from 2 to 9 days (relative to controls). Combining treatments produced dose- and cell line-dependent supra-additive responses. For LNCaP spheroids, the combination of 2 Gy and 100 nM 17AAG resulted in growth delays additive of the treatments individually; however, increasing either the radiation to 6 Gy or the 17AAG concentration to 1000 nM led to synergistic interactions. Similarly, synergy was noted in CWR22Rv1 studies at only 6 Gy and 1000 nM 17AAG. Terminal deoxynucleotidyl transferase-mediated nick end labeling (TUNEL) and Ki67 staining of spheroid sections revealed the increased growth control to be a function of spheroids failing to re-enter the cell cycle. For all 6 Gy experiments, cells remaining from each of the spheroids that failed to regrow were transferred to adherent dishes to evaluate clonogenicity; growth-controlled spheroids also failed to form colonies within 2 weeks of being plated. These results suggest that significant gains in treatment effectiveness may be obtained by combining these treatment modalities, warranting additional preclinical investigation.

INTRODUCTION

With the advent of routine prostate-specific antigen screening, prostate cancer is becoming increasingly detected as localized disease (1). Failure to control the tumor at this level can lead not only to local disease progression, but also to distant metastatic spread (2). Once the disease becomes systemic, it is considered incurable. Biopsy studies and prostate-specific antigen elevation have revealed that the standard dose regimen in prostate cancer RT[1] of 60–70 Gy results in lower cure rates than estimated previously, with 40–60% of patients showing recurrence at 2 years after treatment (3, 4). Efforts to improve outcomes have shifted to a more individualized therapy permitted by more accurate clinical staging and an adapted risk approach (5). In localized therapies, this has translated to dose escalation and intensity modulated RT studies using inverse planning and three-dimensional conformal RT (6, 7). Although increasing the average length of remissions, these studies still fail to consistently provide long-term localized control and also carry an increased risk of late-developing side effects (8–10). Significant improvement to these modalities may be offered by the use of radiosensitizers. In this study we show that the Hsp90 inhibitor, 17AAG, in combination with radiation yields supra-additive growth control in a spheroid system.

17AAG, a derivative of the ansamycin antibiotic geldanamycin, is currently undergoing clinical investigation as a novel antiproliferative agent (11). Eliciting a host of cellular responses, its mechanism of action is mediated through the direct regulation of Hsp90 chaperone protein activity. The drug displaces ATP/ADP at the amino-terminal nucleotide-binding pocket of the chaperone, stabilizing the chaperone-protein complex in a conformation ultimately leading to proteosomal targeting and ubiquitin-mediated degradation (12, 13). Cellular exposure to 17AAG has been correlated with the specific decrease in expression of Hsp90 "client" proteins, primarily receptors and signaling proteins in the tyrosine kinase family, and the upstream dysregulation of their associated pathways (14). Among the most sensitive of these targets are a number of key oncoproteins including Raf-1, HER2, AKT, v-Src, and mutant p-53 (15, 16). Thus, the exact mechanism of 17AAG action will vary dependent on cellular makeup, but has the potential to preferentially regulate the growth of those transformed cells uniquely driven by Hsp90 client proteins and their dependent pathways.

Under specific circumstances, 17AAG is synergistic with chemotherapy. Depending on cell type, combination therapy using low levels of 17AAG was found to enhance the effects of Taxol and doxorubicin on HER2-overexpressing cell lines (17, 18). Both studies attribute the observed synergistic effects at least in part to the direct regulation of HER2 expression by 17AAG treatment. This signaling cascade interacts with both AKT and mitogen-activated protein kinase, proteins critical to a number of tumor proliferation/antiapoptotic pathways (19, 20). Because these pathways are also vital in the cellular response to ionizing radiation, we have investigated the ability of 17AAG to potentiate the effects of radiation therapy in similar cell lines.

Androgen-responsive (LNCaP) and -insensitive (CWR22Rv1) human prostate cancer cell lines were grown as spheroids and used in this study (21, 22). Spheroid cultures have been shown to mimic the three-dimensional organization, differentiated function, and heteroge-

Received 12/3/02; revised 7/31/03; accepted 9/30/03.

Grant support: The CaP CURE Foundation, The Peter M. Sacerdote Foundation, and NIH Grant CA05826.

The costs of publication of this article were defrayed in part by the payment of page charges. This article must therefore be hereby marked *advertisement* in accordance with 18 U.S.C. Section 1734 solely to indicate this fact.

Requests for reprints: George Sgouros, Department of Radiology, Division of Nuclear Medicine, Johns Hopkins Medicine, 220 Ross Research Building, 720 Rutland Avenue, Baltimore, MD 21205. Phone: (410) 614-0116; Fax: (413) 487-3753; E-mail: gsgouro1@jhmi.edu.

[1] The abbreviations used are: RT, radiotherapy; 17AAG, 17-*N*-allylamino-17-demethoxy geldanamycin; Hsp, heat shock protein; TUNEL, terminal deoxynucleotidyl transferase-mediated nick end labeling; AUC, area under the tumor volume curve; LET, linear energy transfer.

neity of intact tissues to a much greater extent than do traditional cell cultures and often exhibit the increased chemo- and radioresistance observed with *in vivo* tumor systems (23–26). Like the *in vivo* systems, *in vitro* spheroids then act as an entity in response to treatment either exhibiting prolonged growth suppression or recovering to resume Gompertzian growth (27). Using this model system we found that acute irradiation and treatment with 17AAG at doses that individually were shown to exhibit only transient growth-controlling properties, when combined, produced supra-additive responses. The results suggest that significant gains in the treatment of localized prostatic tumors may be attained by combining these modalities.

MATERIALS AND METHODS

Cell Culture. The human prostate carcinoma cell line LNCaP (CRL 1740) was purchased from the ATCC (Manassas, VA). CWR22Rv1 cells, human prostatic carcinoma epithelia, were originally provided by Dr. James Jacobberger (Case Western Reserve, Cleveland, OH), and are derived from a xenograft that was serially propagated in mice after castration-induced regression and relapse of the parental, androgen-dependent, CWR22 xenograft (28). Stock T-Flask cultures were propagated at 37°C, 95% relative humidity, and 5% CO_2 in RPMI 1640 (Invitrogen, Carlsbad, CA) supplemented with 10% FCS (Sigma, St. Louis, MO), 100 units/ml penicillin, and 100 mg/ml streptomycin (Gemini Bio-products, Woodland, CA). The medium for CWR22Rv1 culture was adjusted from the above recipe to also contain a total of 2 mM L-glutamine, 1.5 g/liter sodium bicarbonate, 4.5 g/liter glucose, 10 mM HEPES, and 1.0 mM sodium pyruvate (Sigma). Cell concentrations were determined by counting trypsinized cells with a hemocytometer.

Spheroid Initiation. Spheroids were initiated using the liquid-overlay technique of Yuhas *et al.* (29). Details regarding spheroid formation and characterization are described in Ballangrud *et al.* (27). Briefly, liquid overlay plates were prepared from 100-mm or 35-mm Petri dishes (Becton Dickinson Labware, Franklin Lakes, NJ) containing a thin layer of RPMI 1640 solidified with 1% agar (Difco, Detroit, MI). Cell line appropriate medium was inoculated at 6.7×10^4 cells/ml from trypsinized stock cultures. The resulting suspension was used to seed 100-mm plates with $\sim 10^6$ cells. After an incubation of 5–7 days, spheroids of $\sim$200 μm diameter were selected under an inverted phase-contrast microscope (Axiophot 2; Carl Zeiss Ltd., Göttingen, Germany) fitted with an ocular scale using an Eppendorf pipette.

Treatment Protocols. After selection, and between each type of treatment, spheroids were washed three times by suspension in fresh medium. Complete treatment consisted of incubation with 17AAG, irradiation, or a sequential exposure to both. For 17AAG incubation, a 10 mM stock solution in DMSO was serially diluted in medium to produce 1–1000 nM 17AAG and to generate final DMSO concentrations of $<$0.01%. Twelve to 24 washed spheroids were placed in an agar-prepared 35-mm Petri dish as described above and covered with sufficient 17AAG containing medium to cover the entire agar surface. Incubation lasted for 96 h. For irradiation, spheroids were transferred to a 35-mm bacteriological dish in 2 ml of medium and exposed to acute doses of 2, 3, 6, 9, or 12 Gy external beam photon irradiation using a Cesium irradiator at a dose rate of 2.32 Gy/min (Cs-137 Model 68; JL Shepherd and Associates, Glendale, CA).

After complete treatment, washed spheroids were placed in separate agar-prepared wells of a 24-well plate. Untreated spheroids were washed and separated immediately after initial selection. The medium in each well was replaced, and volume measurements performed, twice per week. Using the inverted microscope and ocular scale described previously, the major and minor diameter, d_{max} and d_{min} respectively, were determined and spheroid volume calculated as $V = (1/6) \cdot \pi \cdot d_{max} \cdot d_{min}^2$. Spheroid diameter measurements were initiated on day 0 (treatment start) or day 4 of incubation.

Growth Analysis. For each treatment schedule, at least 12 spheroids were monitored over a maximum of 50 days in duplicate experiments. Measurements were halted either when d_{max} had exceeded the field of view of the microscope at $\times$40 magnification or on spheroid fragmentation into multiple smaller clusters. The median volume at each time point was used to provide a representative characterization of spheroid growth and response. In all of the figures median curves are presented where individual histories are superimposable; where individual curves were not within 1 SD at all of the points, each is presented. Two parameters were used to define treatment response relative to controls and allow comparison of multiple treatments: final volume and growth delay. Final volume, although an independent measure, was reported as a percentage of control final volume. Growth delay was defined as the increase in time, compared with controls, initially required for spheroids to triple in volume from individual starting values.

Immunohistochemistry. Proliferation or apoptosis of tumor cells within spheroids was assessed by Ki67 or TUNEL staining, respectively. At 0, 6, 24, or 48 h after treatment spheroids were washed in cold medium, fixed for 4 h in 4% paraformaldehyde, and placed in paraffin blocks. Serial 5-μm sections of the paraffin blocks were cut using a cryotome and mounted on poly-L-lysine-coated slides that were fixed in hydrogen peroxide and 90% methanol. Ki67 staining was performed using a monoclonal mouse antibody directed against Ki67 and MOM kit (Vector Labs, Burlingame, CA). Apoptotic cells were stained using TUNEL modified from Gavrieli *et al.* (30). Untreated spheroids were used as controls; positive controls were created using DNase I (Boehringer, Ingelheim, Germany). Images were captured digitally from an inverted phase-contrast microscope using a coupled Pixera Professional Camera and associated software (Pixera Visual Communication Suite; Pixera, Los Gatos, CA).

Statistical Analysis. To assess synergy between 17AAG and radiation, the AUC was measured for each spheroid. Synergistic inhibition of tumor growth is defined as the combination treatment group producing on average a smaller log AUC than predicted by the additive model that includes each treatment group separately. We describe this relationship through the inequality:

$$\text{avg}(V \mid S=5M, R=6\ \text{Gy}) < C + \{\text{avg}(V \mid S = 5\mu M, R=0 - C\} + \{\text{avg}(V \mid S=), R=6\ \text{Gy}) - C$$

where V is the log AUC, S = 5 μM and r = 6 Gy represent the doses of 17AAG and radiation used in the experiment, and C is the average log AUC in the control group [C = avg(V | S = 0, r = 0)]. To test for synergy, we computed 2000 bootstrap replicates of the average log AUC, for each of the four groups, and computed the proportion of replicates where the inequality was not obtained. This proportion is termed the achieved significance level (P). A small achieved significance level is an indication that synergistic inhibition of tumor growth has occurred due to the combination treatment.

RESULTS

Response of LNCaP Spheroids to Monotherapy. Initial studies focused on the response of LNCaP spheroids to either 17AAG or radiation exposure. Four-day incubation with increasing doses of 17AAG resulted in a dose-dependent growth delay observed at doses of $\geq$100 nM (Fig. 1). Median growth was unaffected at 1 or 10 nM 17AAG and increasingly delayed from 3.4 to 11 days at 100 and 1000 nM 17AAG, respectively. After these delays, spheroid growth resumed at rates comparable with those observed in untreated controls.

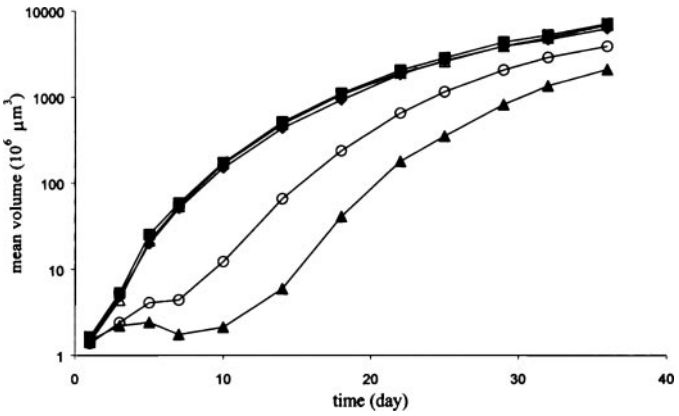

Fig. 1. Median growth of LNCaP human prostate spheroids with 96-h exposure to 17AAG. Median curves were generated from at least 12 individual spheroids: (■) untreated, (△) 1 nM, (♦) 10 nM, (○) 100 nM, and (▲) 1000 nM.

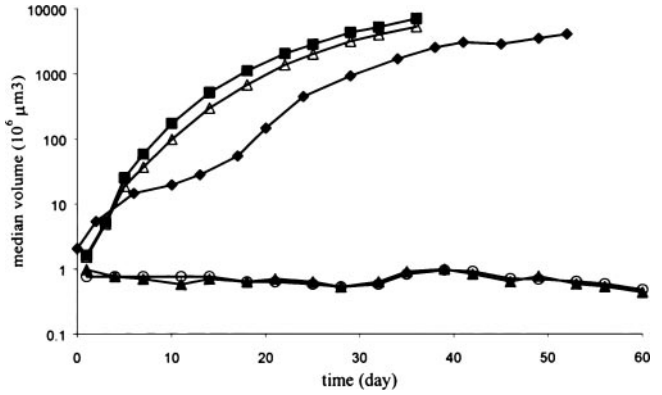

Fig. 2. Median growth of LNCaP human prostate spheroids exposed to acute low-LET irradiation. Median curves were generated from at least 12 individual spheroids. The median growth of control, untreated spheroids is reproduced from Fig. 2 for comparative purposes: (■) untreated, (△) 2 Gy, (♦) 6 Gy, (○) 9 Gy, and (▲) 12 Gy.

Longer delays did, however, correlate with decreased final mean volumes. Spheroids treated with 1000 nM 17AAG achieved a mean volume only 30% that of controls by day 36. Similar transient growth inhibition with recovery was observed when LNCaP spheroids were exposed to acute radiation doses of ≤6 Gy (Fig. 2). Compared with controls, growth was minimally delayed by irradiation to 3 Gy and delayed by 2.6 days at 6 Gy. The higher radiation doses tested, *i.e.*, 9 and 12 Gy, caused complete growth arrest.

Response of LNCaP Spheroids to Combination Therapies. Combination studies investigated the possibility of sensitizing LNCaP spheroids to either radiation or 17AAG effects by alternate treatments of each. Drug exposure began at 100 nM 17AAG, the minimum concentration required to illicit a growth response, and radiation dose was initially set at 2 Gy, the standard clinical dose for fractionated external radiation therapy. Exposure of LNCaP spheroids to 2 Gy and 100 nM 17AAG minimally affected final mean volume and yielded growth delays that were independent of sequence and not significantly greater than the delay due to drug alone ($P < 0.001$); radiation- and drug-first schedules produced median growth delays of 5.1 and 7.6 days, respectively (Fig. 3, *A* and *B*). At 1000 nM 17AAG and 2 Gy, synergistic inhibition of spheroidal growth was observed ($P < 0.001$) regardless of the treatment sequence. Qualitative differences in growth response were, however, found to be dependent on sequence. Radiation first treatments delayed the median growth of LNCaP spheroids an additional 15 days over drug treatment alone and effected a median volume reduction of 77% relative to the same (Fig. 3*A*). When treatments were reversed, 1000 µM 17AAG then 2 Gy, median spheroid growth was essentially halted and median volume remained constant over the observed 54 days (Fig. 3*B*).

When the radiation dose was increased to 6 Gy, both concentrations of 17AAG tested, 100 nM and 1000 nM, yielded synergistic growth control in a schedule-independent manner ($P < 0.001$). However, as in the 2 Gy studies, schedule differences were observed. Six Gy followed by 100 nM 17AAG established a bimodal pattern of response with 2 of 12 LNCaP spheroids exhibiting total growth arrest (Fig. 4*A*). For the reverse treatment, the control ratio doubled to 4 of 12 (Fig. 4*B*). Surviving spheroids resumed robust growth after maximum delays of 35 days. On exposure to 6 Gy then 1000 nM 17AAG, 9 of 12 LNCaP spheroids failed to regrow; the reverse treatment completely arrested all of the spheroids (Fig. 4*C*). For the 6 Gy experiments, cells remaining from each sterilized spheroid were plated on adherent dishes to evaluate remaining clonogenicity. Spheroids that failed to regrow after 6 Gy and 17 AAG combinations also failed to form colonies within 2 weeks of plating.

Time Schedule and Size Effects on Combination Therapy. Treatment schedule was investigated as a possible parameter in the combination response of LNCaP spheroids by sequentially lengthening the interim between the end of 100 nM 17AAG incubation and 6 Gy irradiation. Previously noted increases in treatment effectiveness using drug-first modalities (Fig. 4*B*) were completely abrogated when the interim was increased from 0 to 24 h (Fig. 5).

To ensure that the observed effects were not a result of differences in the number of clonogens within the spheroid and, therefore, an artifact of effective spheroid size at treatment, we examined the radiation or drug response of spheroids with differing initial diameters. Fig. 6*A* shows the effect of size on the growth of LNCaP spheroids irradiated to 6 Gy. In size classes ranging from 150 to 250 µm diameter, spheroids uniformly required <2 days to reach twice their initial volume. However, the smallest class considered, 100 µm diameter, exhibited growth arrest in 3 of 12 spheroids. The same pattern is repeated in Fig. 6*B*, representing the growth response of differently sized spheroids exposed to 1000 nM 17AAG, 96 h. For sizes >100 µm diameter, the growth delay is consistent: 10.4 ± 0.4 days. Again for the smallest class, treatment produced a bimodal outcome with 3 of 12 spheroids growth controlled. In the initial diameter range used for these studies, therefore, the synergistic effects observed with combination therapies are then not simply explained by differences in the number of cells.

Immunohistochemistry. Possible mechanisms governing the observed growth responses were qualitatively assessed using immunohistochemistry. TUNEL and Ki67 staining patterns were used respectively to track alterations in the apoptotic and proliferative state within LNCaP spheroids as a result of differing treatment modalities. Spheroids were sectioned and stained at various times after the end of

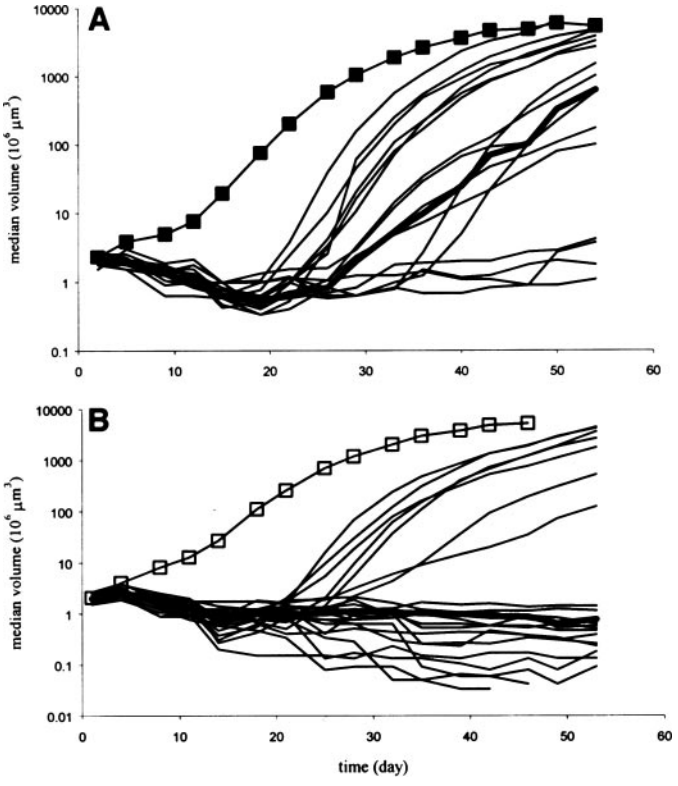

Fig. 3. Individual or median growth curves of LNCaP spheroids exposed to 2 Gy, 17AAG combination therapy. Curves indicated with *symbols* are median values presented where the individual growth curves are superimposable. Median values of graphed individual growth curves are represented in *bold*. *Order in legend description* indicates order in treatment schedule. *A*, (■) 2 Gy, 100 nM 17AAG, (−) 2 Gy, 1000 nM 17AAG; *B*, (□) 100 nM 17AAG, 2 Gy, (−) 1000 nM 17AAG, 2 Gy.

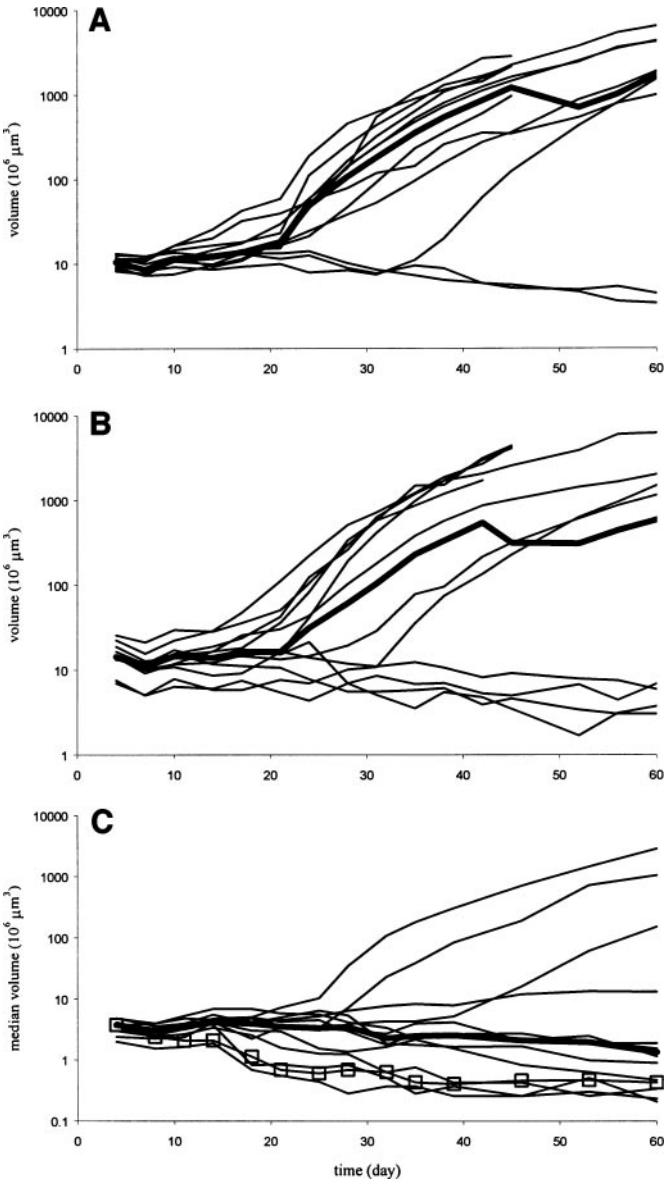

Fig. 4. Individual or median growth curves of LNCaP spheroids exposed to 6 Gy, 17AAG combination therapy. Curves indicated with *symbols* are median values presented where individual growth curves are superimposable. Median values of graphed individual growth curves are represented in *bold*. *Order in legend description* indicates order in treatment schedule. *A*, (−) 6 Gy, 100 nM 17AAG; *B*, (−) 100 nM 17AAG, 6 Gy; *C*, (−) 6 Gy, 1000 nM 17AAG, (□) 1000 nM 17AAG, 6 Gy. Day 0 is the beginning of first treatment for all groups. Some data are presented beginning on day 4, immediately after 17AAG incubation/combination treatment.

incubation with 17AAG, after irradiation to 6 Gy, and after the combination treatment. Fig. 7, *A–C* depicts TUNEL, or apoptotic, staining at 0, 24, and 48 h, respectively, after 1000 nM 17AAG incubation. No clear increase in apoptotic cells was observed with time. This same trend was seen at equal time points after combination treatment, 1000 nM 17AAG +6 Gy irradiation (Fig. 7, *D–F*). Cellular proliferation, however, progressively increased after the end of 17AAG exposure (Fig. 8, *A–C*). Spheroids treated with the combination treatment, 17AAG then radiation, did not exhibit this recovery; the number of proliferating cells remained essentially constant over the times examined (Fig. 8, *D–F*). For all of the image sets, sections obtained at 6 h after treatment were similar to those at 0 h and are not shown.

Response of CWR22Rv1 Spheroids to Monotherapy. A second prostatic cell line, CWR22Rv1, was used to verify the observed effects of 17AAG/radiation combination treatment on spheroids. CWR22Rv1 spheroids exhibited decreased sensitivity to 17AAG and increased sensitivity to radiation as compared with LNCaP spheroids. In contrast to the LNCaP response (Fig. 1), the median growth of the CWR22Rv1 spheroids was not significantly affected by doses to 100 nM 17AAG and delayed by only 8 days at 1000 nM 17AAG (Fig. 9*A*). The radiation response of the two lines was more consistent, essentially paralleling one another at the lowest or highest does tested (Fig. 2; Fig. 9*B*); however, at 6 Gy 22Rv1 spheroids exhibited a growth delay of 12.6 days, six times that observed in LNCaP cultures.

Response of CWR22Rv1 Spheroids to Combination Therapy. Consistent with their relative increase in resistance to 17AAG, synergistic interactions were observed in CWR22Rv1 spheroids at only

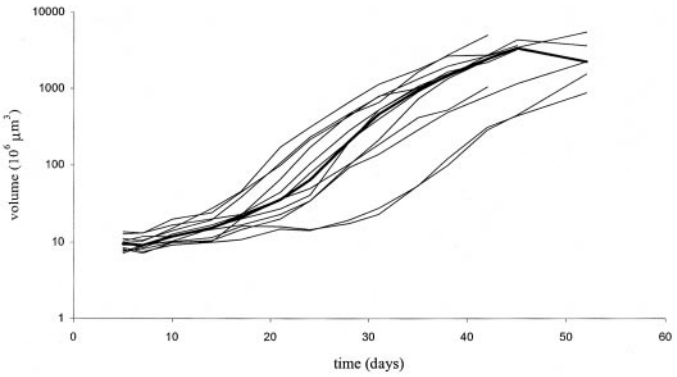

Fig. 5. Individual growth curves of LNCaP spheroids incubated with 100 nM 17AAG followed by 6 Gy. Median values of individual growth curves are represented in *bold*. Interval between 17AAG incubation end and irradiation at 24 h.

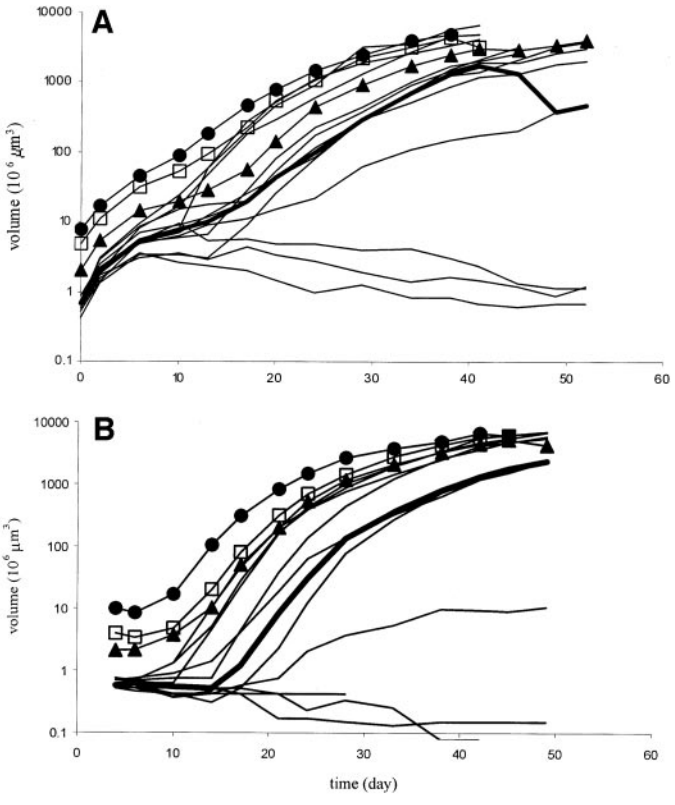

Fig. 6. Individual or median growth curves of differently sized LNCaP spheroids exposed to 6 Gy (*A*) or 1000 nM 17AAG, 96 h (*B*). Curves indicated with *symbols* are median values presented where individual growth curves are superimposable. Median values of graphed individual growth curves are represented in *bold*. Initial diameter of spheroid: (●) 250 µm, (□) 200 µm, (▲) 150 µm, (−) 100 µm.

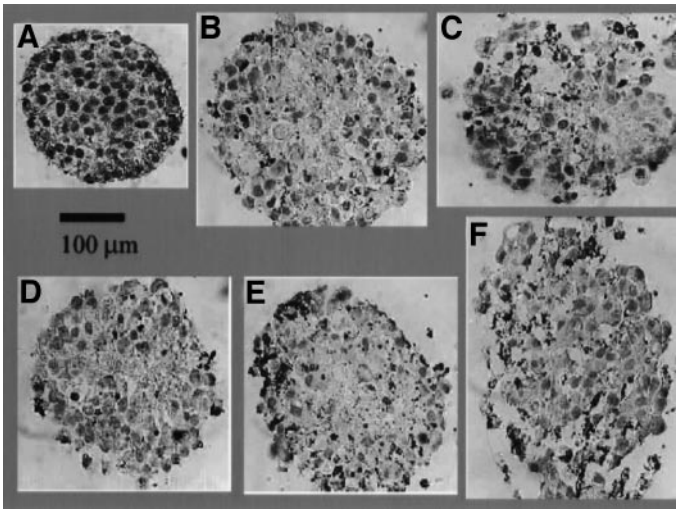

Fig. 7. TUNEL staining of spheroid sections depicting apoptotic cells (*black color*) at 0 (*A*), 24 (*B*), and 48 (*C*) h after the end of a 96 h exposure to 1 μM 17-AAG. *D–F* also show apoptotic staining at the times listed above, but for spheroids treated with 17-AAG (1 μM, 96 h) and then immediately irradiated to 6 Gy. Slight distortion of spheroid structure and shape due to sectioning are noted. *Scale bar* is accurate for all panels.

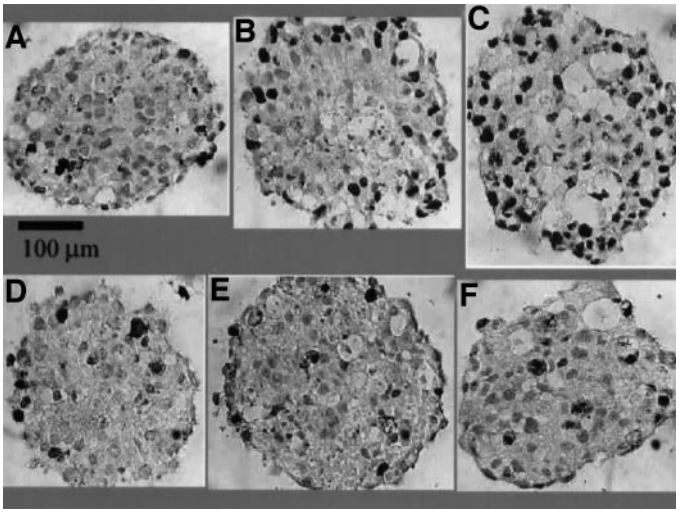

Fig. 8. Ki67 staining of spheroid sections depicting proliferating cells (*black color*) at 0 (*A*), 24 (*B*), and 48 (*C*) h after the end of a 96 h exposure to 1 μM 17-AAG. *D–F* also show staining for cell proliferation at the times listed above but for spheroids treated with 17-AAG (1 μM, 96 h) and then immediately irradiated to 6 Gy. Slight distortion of spheroid structure and shape due to sectioning are noted. *Scale bar* is accurate for all panels.

the highest levels of drug tested and then only in a sequence-dependent manner. The response of CWR22Rv1 spheroids did not change significantly when radiation monotherapy was combined with 100 nM 17AAG (Fig. 10*A*). Immediately after irradiation these spheroids grew rapidly for 3 days then entered a transient growth arrest that lasted for 6 days, regardless of sequence. Earlier delays did, however, correlate with decreased final median volumes: radiation-first treatments resulted in 22Rv1 spheroids that were 50% smaller than those generated by the reverse experiments. Increasing 17AAG concentration to 1000 nM resulted in synergistic interaction for only drug-first schedules ($P < 0.001$; Fig. 10*B*). The sequence 1000 nM 17AAG followed by 6 Gy caused complete growth arrest in 8 of 12 spheroids; in contrast, using radiation first in the same combination delayed median growth by 12.5 days and resulted in no arrest. As with the 6 Gy LNCaP combination experiments, CWR22Rv1 spheroids that failed to grow in combination treatments also failed to form colonies in outgrowth assays.

DISCUSSION

Numerous studies have examined the possibility of combining RT with radiosensitizing agents to enhance patient response (reviewed in Ref. 31). Two general classes of agents have been considered: hypoxic cell sensitizers, such as the nitroimidazoles, and the various chemotherapeutics including DNA intercalators, microtubule stabilizers, and metabolic inhibitors (32). 17AAG belongs neither to the different categories of conventional chemotherapeutics listed above nor is it dependent on the presence of hypoxic cells. With this study, however, we have demonstrated that low-level treatment with 17AAG synergistically interacts with ionizing radiation in prostate carcinoma spheroids.

The levels of 17AAG tested produced at most transient effects in spheroid growth consistent with its highly reversible nature (33, 34). LNCaP spheroids were found to be more sensitive to its growth-controlling and radiosensitizing properties than spheroids of CWR22Rv1 cells. Observed differences in sensitivity may be partially explained by the greater relative HER-2/*neu* expression of LNCaP cells (22). Münster *et al.* (35) have shown a positive correlation between HER-2/*neu* expression and 17AAG sensitivity. Correspondingly, CWR22Rv1 spheroids exhibited the enhanced effects of combination therapy at only the highest combination of 17AAG tested: 10-fold greater than that required for the same effect in LNCaP studies.

The mechanism through which 17AAG and radiation interact is not clear. In breast cancer cell lines, 17AAG in combination with Taxol, a proliferation-dependent cytotoxin, yielded highly sequence-dependent effects (16). 17AAG exposure before Taxol arrested cells in G_1,

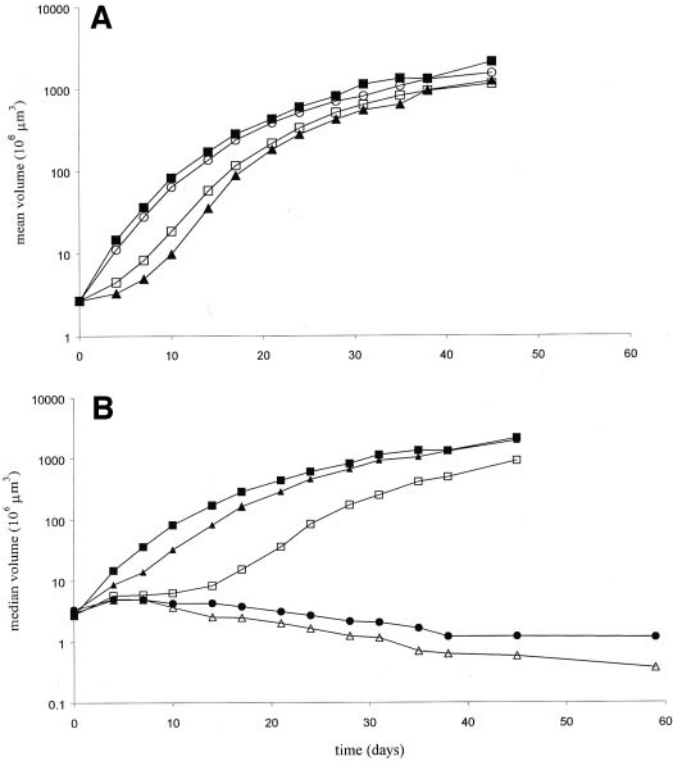

Fig. 9. Median growth of CWR22R-v1 human prostate spheroids with (*A*) 96 h exposure to 17AAG: (■) untreated, (♦) 10 nM, (○) 100 nM, (▲) 1000 nM, or (*B*) acute exposure to low-LET irradiation: (■) untreated, (○) 2 Gy, (□) 6 Gy, (●) 9 Gy, (△) 12 Gy. Median curves were generated from at least 12 individual spheroids.

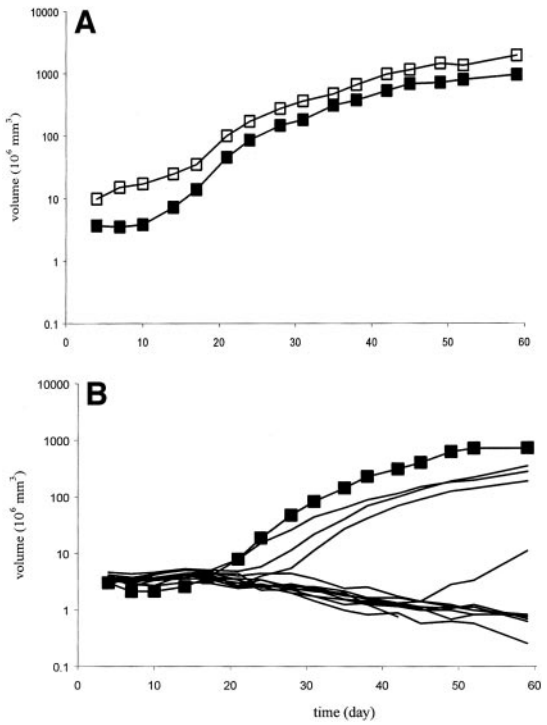

Fig. 10. Individual or median growth curves of CWR22R-v1 spheroids exposed to 6 Gy, 17AAG combination therapy. Curves indicated with *symbols* are median values presented where individual growth curves are superimposable. Median values of graphed individual growth curves are represented in *bold*. *Order in legend labels* indicates order in treatment schedule. *A*, (■) 6 Gy, 100 nM 17AAG, (□) 100 nM, 6Gy; (*B*) (■) 6 Gy, 1000 nM 17AAG, (−)1000 nM 17AAG, 6 Gy.

abrogating the cytotoxic effects of the drug; incubation after Taxol was synergistic. Although radiation effects are also dependent on cellular cycling no such antagonism was observed in our studies. Whereas G_1-blocked cells are known to be radioresistant (36), it is unknown if our spheroidal cells are similarly blocked as indicated by immunohistochemistry. After the removal of 17AAG, it is interesting that both the proliferative and apoptotic markers of drug-only treated spheroids follow the same pattern, appearing first at the periphery and moving to the interior with time. This likely represents the diffusion of drug out of the spheroid and the return of native cell function. Sufficiently damaged cells become apoptotic and perhaps necrotic only on attempting to re-enter the cell cycle. As compared with surface cells, possible delays in the appearance of either marker in the spheroid interior may also reflect their relatively slower proliferation rate. Ultimately, the balance of viable/apoptotic cells will determine the fate of the spheroid as an entity. As indicated in our volumetric controls, below some threshold number of active cells the spheroid will not grow. Although sufficient to explain the bimodal outcomes of many of our treatment combinations, this is likely not the scenario observed in the spheroids growth-controlled by the synergistic combinations. Immunohistochemistry suggests that growth control of spheroids exposed to the combinations is not mediated through enhanced apoptosis or a minority of cycling cells, but rather by a block to proliferation. This is perhaps best explained by the general dysregulation of stress, proliferation, and repair-related elements caused by 17AAG exposure, rendering target cells uniformly more susceptible to subsequent toxic insult and thereby reducing the threshold for repairable, radiation-induced damage (12).

A substantial therapeutic ratio has been achieved in both animal and patient studies with 17AAG alone. In combination with radiation we have observed therapeutic effects at radiation and 17AAG doses that are not therapeutic individually. This suggests that the combination of 17AAG with RT or targeted radionuclide therapy is likely to yield substantial therapeutic enhancement with minimal increases in toxicity.

Using drug and radiation levels that minimally impacted spheroid growth individually, we have demonstrated supra-additive improvements in both spheroid volume control and sterilization ratio with combination therapies in prostate carcinoma spheroids. The spheroid system recapitulates, *in vitro*, many of the essential elements of micrometastatic tumors and has been repeatedly shown to better represent responses observed *in vivo*. The possibility of combining 17AAG with conformal, intensity-modulated inverse planning approaches or with targeted radionuclide therapy promises the potential for improved local and metastatic control of prostate cancer.

REFERENCES

1. Stanford, J. L., Stephenson, R. A., Coyle, L. M., Cerhan, J., Correa, R., Eley, J. W., Gilliland, F., Hankey, B., Kolonel, L. N., Kosary, C., Ross, R., Severson, R., and West, D. Prostate Cancer Trends 1973–1995, SEER Program, National Cancer Institute. NIH Pub. No. 99–4543. Bethesda, MD, 1999.
2. Coen, J. J., Zietman, A. L., Thakral, H., and Shipley, W. U. Radical radiation for localized prostate cancer: local persistence of disease results in late wave of metastases. J. Clin. Oncol., *20:* 3199–3205, 2002.
3. Ljung, G., Norberg, M., Hansson, H., de la Torre, M., Egevad, L., and Holmberg, L. Transrectal ultrasonically-guided core biopsies in the assessment of local cure of prostatic cancer after radical external beam radiotherapy. Acta Oncol., *34:* 945–952, 1995.
4. Scardino, P. T., and Wheeler, T. M. Local control of prostate cancer with radiotherapy: frequency and prognostic significance of positive results of postirradiation prostate biopsy. NCI Monogr., 95–103, 1988.
5. Morris, M. J., and Scher, H. I. Novel strategies and therapeutics for the treatment of prostate carcinoma. Cancer (Phila.), *89:* 1329–1348, 2000.
6. Bogers, J. A., van der Maazen, R. W., and Visser, A. G. Conformal photon-beam radiotherapy of prostate carcinoma. Eur. Urol., *41:* 515–522, 2002.
7. Zelefsky, M. J., Fuks, Z., Happersett, L., Lee, H. J., Ling, C. C., Burman, C. M., Hunt, M., Wolfe, T., Venkatraman, E. S., Jackson, A., Skwarchuk, M., and Leibel, S. A. Clinical experience with intensity modulated radiation therapy (IMRT) in prostate cancer. Radiother. Oncol., *55:* 241–249, 2000.
8. Zelefsky, M. J., Fuks, Z., Hunt, M., Lee, H. J., Lombardi, D., Ling, C. C., Reuter, V. E., Venkatraman, E. S., and Leibel, S. A. High dose radiation delivered by intensity modulated conformal radiotherapy improves the outcome of localized prostate cancer. J. Urol., *166:* 876–881, 2001.
9. Skwarchuk, M. W., Jackson, A., Zelefsky, M. J., Venkatraman, E. S., Cowen, D. M., Levegrun, S., Burman, C. M., Fuks, Z., Leibel, S. A., and Ling, C. C. Late rectal toxicity after conformal radiotherapy of prostate cancer (I): multivariate analysis and dose-response. Int. J. Radiat. Oncol. Biol. Phys., *47:* 103–113, 2000.
10. Zelefsky, M. J., Cowen, D., Fuks, Z., Shike, M., Burman, C., Jackson, A., Venkatramen, E. S., and Leibel, S. A. Long term tolerance of high dose three-dimensional conformal radiotherapy in patients with localized prostate carcinoma. Cancer (Phila.), *85:* 2460–2468, 1999.
11. Adams, J., and Elliot, P. J. New agents in cancer clinical trials. Oncogene, *19:* 6687–6692, 2000.
12. Neckers, L., Schulte, T. W., and Mimmaugh, E. Geldanamycin as a potent anti-cancer agent: its molecular target and biochemical activity. Investig. New Drugs, *17:* 361–373, 1999.
13. Schneider, C., Sepp-Lorenzino, L., Nimmesgern, E., Ouerfelli, O., Danishefsky, S., Rosen, N., and Harlt, F. U. Pharmacologic shifting of a balance between protein refolding and degradation mediated by Hsp90. Proc. Natl. Acad. Sci. USA, *93:* 14536–14541, 1996.
14. Pearl, L. H., and Prodromou, C. Structure and *in vivo* function of Hsp 90. Curr. Opin. Struct. Biol., *10:* 46–51, 2000.
15. Blagosklonny, M. V. Hsp-90-associated oncoproteins: multiple targets of geldanamycin and its analogs. Leukemia (Baltimore), *16:* 455–462, 2002.
16. Neckers, L. Hsp90 inhibitors as novel cancer chemotherapeutic agents. Trends Mol. Med., *8:* S55–S61, 2002.
17. Münster, P. N., Basso, A., Solit, D., Norton, L., and Rosen, N. Modulation of Hsp90 function by ansamycins sensitizes breast cancer cells to chemotherapy-induced apoptosis in an RB-and schedule-dependent manner. Clin. Cancer Res., *7:* 2228–2236, 2001.
18. Nguyen, D. M., Chen, A., Mixon, A., Schrump, D. S., and Roth, J. A. Sequence-dependent enhancement of paclitaxel toxicity in non-small cell lung cancer by 17-allyamino 17-demethoxygelanamycin. J. Thorac. Cardiovasc. Surg., *118:* 908–915, 1999.
19. Wen, Y., Hu, M. C., Makino, K., Spohn, B., Bartholomeusz, G.,. Yan, D. H., and Hung, M. C. Her-2/neu promotes androgen independent survival and growth of prostate cells through the AKT pathway. Cancer Res., *60:* 6841–6845, 2000.
20. Yeh, S., Lin, H. K., Kang, H. Y., Thin, T. H., Lin, M. F., and Chang, C. From Her2/Neu signal cascade to androgen receptor and its coactivators: a novel pathway by induction of androgen target genes through MAP kinase in prostate cancer cells. Proc. Natl. Acad. Sci. USA, *96:* 5458–5463, 1999.
21. Agus, D. B., Cordon-Cardo, C., Fox, W., Drobnjak, M., Koff, A., Golde, D. W., and Scher, H. I. Prostate Cancer cell cycle regulators: response to androgen withdrawal

and development of androgen independence. J. Natl. Cancer Inst., *91:* 1896–1876, 1999.
22. Agus, D. B., Scher, H. I., Higgins, B., Fox, W. D., Heller, G., Fazzari, M., Cordon-Cardo, C., and Golde, D. W. Response of prostate cancer to anti-Her-2/neu antibody in androgen-dependent and -independent human xenograft models. Cancer Res., *59:* 4761–4764, 1999.
23. Wartenburg, M., Frey, C., Diedershagen, H., Ritgen, J., Heschler, J., and Sauer, H. Development of an intrinsic P-glycoprotein-mediated doxorubicin resistance in quiescent cell layers of large, multicellular prostate tumor spheroids. Int. J. Cancer, *75:* 855–863, 1998.
24. St. Croix, B., and Kerbel, R. S. Cell adhesion and drug resistance in cancer. Curr. Opin. Cell Biol., *9:* 549–556, 1997.
25. Santini, M. T., Rainaldi, G., and Indovina, P. L. Multicellular tumor spheroids in radiation biology. Int. J. Radiat. Biol., *75:* 787–799, 1999.
26. Charlton, D. E. The survival of monolayers of cells growing in clusters irradiated by ^{211}At appended to the cell surfaces. Radiat. Res., *151:* 750–753, 1999.
27. Ballangrud, A. M., Yang, Y. H., Dnistrian, A., Lampen, N. M., and Sgouros, G. Growth and characterization of LNCaP prostate cancer cell spheroids. Clin. Cancer Res., *5:* 3171s–3176s, 1999.
28. Sramkoski, R. M., Pretlow, T. G. 2nd, Gianconia, J. M., Pretlow, T. P., Schwartz, S., Sy, M. S., Marengo, S. R., Rhim, J. S., Zhang, D., and Jacobberger, J. W. A new human prostate carcinoma cell line, 22Rv1. In Vitro Cell. Dev. Biol. Anim., *35:* 403–409, 1999.
29. Yuhas, J. M., Li, A. P., Martinez, A. O., and Ladman, A. J. A simplified method for production and growth of multicellular spheroids. Cancer Res., *37:* 3639–3643, 1977.
30. Gavrieli, Y., Sherman, Y., and Ben-Sasson, S. A. Identification of programmed cell death is situ via specific labeling of nuclear DNA fragmentation. J. Cell. Biol., *119:* 493–501, 1992.
31. Senzer, N. Prostate cancer: multimodality approaches with docetaxel. Semin. Oncol., *28:* 77–85, 2002.
32. Inanami, O., Sugihara, K., Okui, T., Haysahi, M., Tsujitani, M., and Kuwabara, M. Hypoxia and etanidazole alter radiation-induced apoptosis in HL60 cells but not in MOLT-4 cells. Int. J. Radiat. Biol., *78:* 267–274, 2002.
33. Solit, D. B., Zheng, F. F., Drobnjak, M., Münster, P. N., Higgins, B., Verbel, D., Heller, G., Tong, W., Cordon-Cardo, C., Agus, D. B., Scher, H. I., and Rosen, N. 17-allyamino-17demethoxygeldanamycin induces the degradation of androgen receptor and HER-2/*neu* and inhibits the growth of prostate cancer xenografts. Clin. Cancer Res., *8:* 986–993, 2002.
34. Münster, P. N., Srethapakdi, M., Moasser, M. M., and Rosen, N. Inhibition of heat shock protein 90 function by ansamycins causes the morphological and functional differentiaion of breast cancer cells. Cancer Res., *61:* 2945–2952, 2001.
35. Münster, P. N., Marchion, D. C., Basso, A. D., and Rosen, N. Degradation of HER2 by ansamycins induces growth arrest and apoptosis in cells with HER2 overexpression via HER3, phosphatidylinositol 3′-kinase-AKT-dependent pathway. Cancer Res., *62:* 3132–3137, 2002.
36. Hall, E. J. Radiobiology for the Radiologist, 4th Edition, pp. 97–100. Philadelphia: Harper & Row Publishers, 1994.